Stability Analysis of Rotors using Three-Dimensional Finite Elements and HRZ Mass Lumping Scheme

Smitadhi Ganguly, A.Nandi , S.Neogy

Abstract

The present work aims at eigenvalue analysis of three-dimensional finite element rotor models using a simple mass-lumping scheme frequently used in structural dynamics. Finite element analysis of spinning systems is more complicated than the conventional structural ones due to the presence of the anti-symmetric gyroscopic or Coriolis matrices. In the present work, the mass matrix is lumped keeping the gyroscopic/Coriolis matrix intact. Unlike structural dynamics, in order to take care of the anti-symmetric terms the eigenvalue analysis needs to be performed in state space. For rotors on isotropic or rigid bearings, the matrices in the state space becomes $2n \times 2n$ in size, where the mass, stiffness and gyroscopic/Coriolis matrices are of the order $n \times n$. If the bearings are orthotropic, the size of the eigenvalue problem further increases depending on the terms considered in the assumed solution. In this case the mass matrix appears twice in the final eigenvalue problem and only one of them requires to be lumped. It is shown in this work that in both the above cases, a diagonal mass matrix considerably reduces the computational effort. It is observed that the results using conventional and lumped mass matrices match particularly well when the rotor has different bending stiffness in two perpendicular planes.

1 Introduction

The research endeavor in this direction started with Rayleigh and Timoshenko beam elements [1] for shaft and point inertia elements for discs. Though these elements are still very popular in practice, researchers extensively experimented with conical shaft elements, axisymmetric rotor elements and three-dimensional solid elements [2,3,4,5]. As the finite element models became more and more complicated over years, the number of degrees of freedom involved also increased manifold.

The present work deals with an aspect of analysis of three-dimensional analysis of rotor models using 10-node tetrahedral elements. In three-dimensional formulation one has to use a spinning frame for derivation of the governing equations [5]. In this spinning frame, the orthotropic bearing stiffness becomes periodic. The governing equations thus become parametric in nature. A rotor cross-section is symmetric when the rotor has same bending stiffness in two perpendicular planes. A symmetric rotor on rigid, isotropic and orthotropic bearing is stable in absence of a destabilizing source like rotating damping, oil seals etc. A non-symmetric rotor is unstable in a specific region of spin speed [6].

Smitadhi Ganguly
Hooghly Engineering & Technology College, P.O. & Dist. Hooghly, Pin 712103, West Bengal

A.Nandi
Mechanical Engineering Det., Jadavpur University, Kolkata 700 032, E-mail:nandi.arghya@gmail.com

S.Neogy
Mechanical Engineering Det., Jadavpur University, Kolkata 700 032

The present work explores the possibility of using the HRZ lumping scheme [7] in eigenvalue analysis of three-dimensional finite element model of rotors. Campbell diagrams are constructed for symmetric rotors on rigid/isotropic bearings using consistent and lumped mass matrices and compared. For non-symmetric rotors on rigid/isotropic bearings both real and imaginary part of the eigenvalues are compared. Results for several test cases are presented where rotors with circular, square, rectangular and elliptic cross-sections are considered.

For stability analysis of rotors on orthotropic bearings, a variant of the Hill's method is adopted in this work [8]. This method reduces the problem to computation of eigenvalues of a parametric system. This problem is ultimately converted to a generalized eigenvalue problem with much larger number of degrees of freedom. The HRZ scheme makes the original mass matrix a diagonal one. When stability analysis is performed in state-space, a diagonal mass matrix enables one to convert this generalized eigenvalue problem of this much larger system to a standard one. The mass matrix occur a couple of times in the final eigenvalue problem. A lumped mass matrix is used for one and a consistent one for the other. Now, the user has to store and operate on much less number of terms. For this case, since the work is still in progress, the authors could only present the formulation part.

2 Analysis

In a spinning frame, the finite element equations for a three-dimensional rotor model supported on an orthotropic spring can be written as follows[8]:

$$[M_r]\{\ddot{U}\}+[C_r]\{\dot{U}\}+\left([K_r]_{wb}+[K_0]_b+[K_c]_b\cos(2\Omega t)+[K_s]_b\sin(2\Omega t)\right)\{U\}=\{f\} \qquad (1)$$

$[K_r]_{wb}$ =Appropriate stiffness matrix plus part of isotropic support damping in rotating frame without considering the boundary (support) stiffness contributions

$[K_0]_b$ = Matrix having non-zero contributions from support stiffness terms, which are not functions of time

$[K_c]_b, [K_s]_b$ = Matrix having non-zero contributions from support stiffness terms, which are coefficients of cosine and sine functions respectively

In state vector form,

$$\begin{bmatrix}[M_r] & [0]\\ [0] & [I]\end{bmatrix}\begin{Bmatrix}\{\ddot{U}\}\\ \{\dot{U}\}\end{Bmatrix}+\begin{bmatrix}[C_r] & [K_r]_{wb}+[K_0]_b\\ -[I] & [0]\end{bmatrix}\begin{Bmatrix}\{\dot{U}\}\\ \{U\}\end{Bmatrix}+\begin{bmatrix}[0] & [K_c]_b\\ [0] & [0]\end{bmatrix}\cos 2\Omega t\begin{Bmatrix}\{\dot{U}\}\\ \{U\}\end{Bmatrix}+$$
$$\begin{bmatrix}[0] & [K_S]_b\\ [0] & [0]\end{bmatrix}\sin 2\Omega t\begin{Bmatrix}\{\dot{U}\}\\ \{U\}\end{Bmatrix}=\begin{Bmatrix}\{0\}\\ \{0\}\end{Bmatrix}------(2)$$

Equation (2) is written as follows: -

$$[\overline{M}]\{\dot{Z}\}+[\overline{K}]\{Z\}+[\overline{K}_C]\cos 2\Omega t\{Z\}+[\overline{K}_S]\sin 2\Omega t\{Z\}=\{0\} \qquad (3)$$

For rotor on rigid/isotropic bearing, $[\overline{K}_C]=[\overline{K}_S]=[0]$

Therefore, one obtains a generalized eigenvalue problem,

$$\left[\overline{K}\right]\left\{Z\right\} = -\lambda\left[\overline{M}\right]\left\{\dot{Z}\right\} \tag{4}$$

The diagonal mass matrix is denoted by the symbol $\left\lfloor (m_r)_{ii} \right\rfloor$

$$\begin{bmatrix} \left[\dfrac{1}{(m_r)_{ii}}\right]\left[C_r\right] & \left[\dfrac{1}{(m_r)_{ii}}\right]\left(\left[K_r\right]_{wb} + \left[K_0\right]_b\right) \\ -\left[I\right] & \left[0\right] \end{bmatrix} \begin{Bmatrix} \{\dot{U}\} \\ \{U\} \end{Bmatrix} = -\lambda \begin{Bmatrix} \{\dot{U}\} \\ \{U\} \end{Bmatrix} \tag{5}$$

Where, $\left[\dfrac{1}{(m_r)_{ii}}\right]$ is a another diagonal matrix whose diagonal elements are reciprocal of those of $\left[(m_r)_{ii}\right]$

For rotor on orthotropic bearing, a solution of the equation (3) can be assumed in the following form: -

$$\left\{Z\right\} = \left\{y(t)\right\}e^{\lambda t} \tag{6}$$

Where,

$$\left\{y(t)\right\} = \left\{a_0\right\} + \left\{a_2\right\}\cos 2\Omega t + \left\{b_2\right\}\sin 2\Omega t + \left\{a_4\right\}\cos 4\Omega t + \left\{b_4\right\}\sin 4\Omega t \tag{7}$$

Substituting relation (7) in equation (3) the following set of homogeneous first order ordinary differentials equations are obtained.

$$\left[\overline{M}\right]\left\{y\right\} + \lambda\left[\overline{M}\right]\left\{y\right\} + \left[\overline{K}\right]\left\{y\right\} + \left[\overline{K}_c\right]\cos 2\Omega t\left\{y\right\} + \left[\overline{K}_s\right]\sin 2\Omega t\left\{y\right\} = \left\{0\right\} \tag{8}$$

A single element in the $\left\{y\right\}$ vector can be represented as

$$y_k = a_0^{\ k} + a_2^{\ k}\cos 2\Omega t + b_2^{\ k}\sin 2\Omega t + a_4^{\ k}\cos 4\Omega t + b_4^{\ k}\sin 4\Omega t$$

This can be written as

$$y_k = \left\lfloor T \right\rfloor\left\{d^k\right\} = T_j d_j^{\ k} \tag{9}$$

Where,

$$\left\lfloor T \right\rfloor = \left\lfloor 1 \quad \cos 2\Omega t \quad \sin 2\Omega t \quad \cos 4\Omega t \quad \sin 4\Omega t \right\rfloor$$

$$\left\{d^k\right\} = \left\lfloor a_0^{\ k} \quad a_2^{\ k} \quad b_2^{\ k} \quad a_4^{\ k} \quad b_4^{\ k} \right\rfloor^T$$

Now,

$$\dot{y}_k = \dot{T}_j d_j^{\ k} = T_i D_{1ij} d_j^{\ k} \tag{10}$$

Where, the matrix $\left[D_1\right]$ is the first order differentiation operation matrix

Neglecting coefficients of the terms $\cos 6\Omega t$ and $\sin 6\Omega t$, the product $y_k \cos 2\Omega t$ can be expressed as follows: -

$$y_k \cos 2\Omega t = T_i P_{cij} d_j^k \tag{11}$$

Where, the matrix $\left[P_c\right]$ is the product operation matrix for stiffnesses with cosine coefficients.

Similarly, the product $y_k \sin 2\Omega t$ can be expressed as follows: -

$$y_k \sin 2\Omega t = T_i P_{sij} d_j^k \tag{12}$$

Where, the matrix $\left[P_s\right]$ is the product operation matrix for stiffnesses with sine coefficients.

Equation (8) can be expressed in indicial notation as follows: -

$$\overline{m}_{ij}\dot{y}_j + \lambda\overline{m}_{ij}h_j + \overline{k}_{ij}y_j + \overline{k}_{cij}\cos 2\Omega t y_j + \overline{k}_{sij}\sin 2\Omega t y_j = 0 \tag{13}$$

Replacing y_j by its assumed solution as given in equation (6) and making use of the first order differentiation operation matrix and the product operation matrices for cosine and sine terms, the following expression is obtained.

$$\overline{m}_{ij}T_k D_{1kl} d_l^{\;j} + \lambda\overline{m}_{ij}T_k d_k^{\;j} + \overline{k}_{ij}T_k d_k^{\;j} + \overline{k}_{cij}T_k P_{ckl} d_l^{\;j} + \overline{k}_{sij}T_k P_{skl} d_l^{\;j} = 0$$

Or,

$$T_k m_{ij} D_{1kl} d_l^{\;j} + \lambda T_k \overline{m}_{ij}\delta_{kl} d_l^{\;j} + T_k \overline{k}_{ij}\delta_{kl} d_l^{\;j} + T_k \overline{k}_{cij} P_{ckl} d_l^{\;j}$$

$$+ T_k \overline{k}_{sij} P_{skl} d_l^{\;j} = 0 - - - (14)$$

Finally one obtains,

$$\left[A\right]\left\{X\right\} = -\lambda\left[B\right]\left\{X\right\} \tag{15}$$

Where,

$$\left[A\right] = \left(\left[\overline{M}\right]\otimes\left\lfloor D_1\right\rfloor + \left[\overline{K}\right]\otimes\left[I\right] + \left[\overline{K}_c\right]\otimes\left[P_c\right] + \left[\overline{K}_s\right]\otimes\left[P_s\right]\right)$$

$$\left[B\right] = \left[\overline{M}\right]\otimes\left[I\right]$$

$$\left\{X\right\} = \begin{Bmatrix} \left\{d^1\right\} \\ \left\{d^2\right\} \\ - \\ - \end{Bmatrix}$$

The Kronecker product between two matrices $\left[A\right]$ and $\left[B\right]$ is defined as follows: -

$$\left[A\right]\otimes\left[B\right] = \begin{bmatrix} a_{11}\left[B\right] & a_{12}\left[B\right] & - & - \\ a_{21}\left[B\right] & a_{22}\left[B\right] & - & - \\ - & - & - & - \\ - & - & - & - \end{bmatrix} \tag{16}$$

In equation one can use a lumped mass matrix in the right hand side and a consistent one in left hand one.

The right hand side now becomes $\begin{bmatrix} \left[\left(m_r\right)_{ii}\right] & \left[0\right] \\ \left[0\right] & \left[I\right] \end{bmatrix}\otimes\left[I\right] = \left[\left(b\right)_{ii}\right]$

Equation becomes

$$\left[\left(\frac{1}{b}\right)_{ii}\right][A]\{X\} = -\lambda\{X\} \tag{17}$$

Where, the matrices $\left[(b)_{ii}\right]$ and $\left[\left(\frac{1}{b}\right)_{ii}\right]$ are both diagonal matrices. Diagonal element of one is the reciprocal of the corresponding one of the other.
In general, the eigenvalues are complex numbers whose imaginary parts are the whirl frequencies and the real parts decide stability. A positive real part of an eigenvalue indicates instability of that mode.

2.1 HRZ lumping scheme

The HRZ scheme is a simple and effective scheme [7] for producing a diagonal mass matrix for structural dynamic analysis. The basic idea is to use the scaled diagonal terms of the consistent mass matrix. The scaling is so done that the total mass of the element is preserved. The scale factor is determined by dividing the total mass by the sum of the diagonal terms associated with a translational degree of freedom.

3 Case Studies

The finite element mesh is created using 10-node tetrahedral element, which is better suited for meshing solids with irregular shape than the hexahedral brick element. With hexahedral elements it is very difficult to mesh the region where the shaft is connected to the disc.

The eigenvalues are computed for different rotor configurations using consistent and lumped mass matrices. It is known that the first mode of the rotor can be accurately modelled using a fairly coarse mesh. In the present work, for selection of the mesh, a convergence study on the first two eigenvalues is performed. In order to model a fixed end of a cantilever all the degrees of freedom at the fixed end are restrained. The zero slope condition is achieved by restraining the axial degrees of freedom.

First,a cantilevered shaft-disc system is considered (Fig.1). The shaft is of 400 mm length and 10 mm radius. The disc has a radius of 100 mm and thickness of 10 mm. The system is modelled using 10 node tetrahedral elements. The whirl speed is plotted against spin speed of the rotor in Fig.3. For the forward whirl speeds the results from the two formulations are very close but for the backward whirl speeds the results deviate more with the lumped mass formulation predicting lower values.

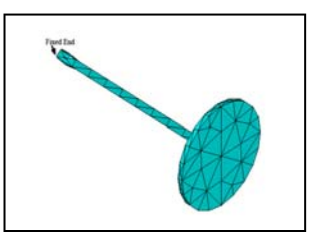

Fig. 1: Mesh idealization for shaft-disc system

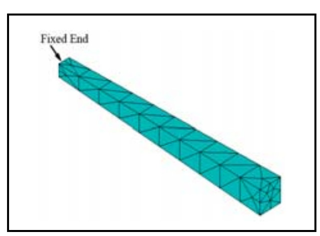

Fig. 2: Mesh idealization for tapered square shaft

In the second numerical example, a cantilevered tapered shaft with square cross section is considered (Fig.2). The shaft has 20 mm × 20 mm square cross section and a length of 400 mm. The finite element mesh is shown in Figure. The results deviate considerably specially for the backward whirl (Fig.4).

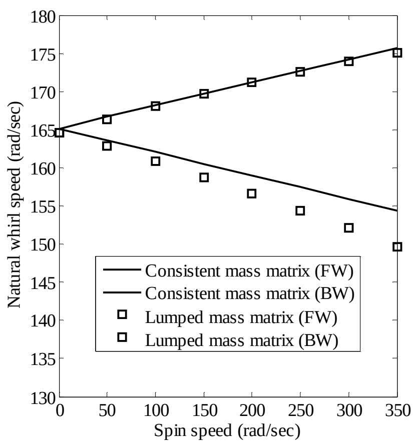

Fig. 3: Campbell diagram for shaft-disc system

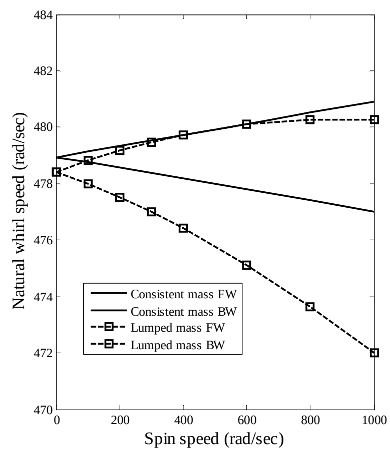

Fig. 4: Campbell diagram for tapered square shaft

It is known that a rotor with different bending stiffness in two perpendicular planes is unstable. In this example stability analysis of a cantilevered tapered shaft of rectangular cross section is carried out with both consistent mass matrix and lumped mass matrix formulations. The shaft is 400 mm long and tapers from a 60 mm × 40 mm cross section to a cross section with half the dimensions (Fig. 5). The smaller end is fixed. The real and imaginary parts of the eigenvalues are plotted in Figure 7 & Figure 8. The value of the maximum real part of eigenvalues indicates stability.. The same configuration with 80 mm × 40 mm cross-section at the left end is analyzed next (Fig. 6) and the results are plotted in Figure 9 & Figure 10. The consistent and lumped formulations give almost identical results and the values are in agreement with the values given in standard literature.

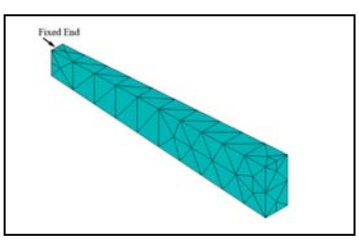

Fig. 5: Mesh idealization for tapered rectangular shaft with 60 mm × 40 mm cross section

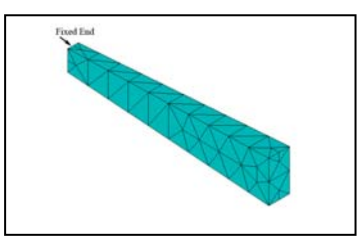

Fig. 6: Mesh idealization for tapered rectangular shaft with 80 mm × 40 mm cross section

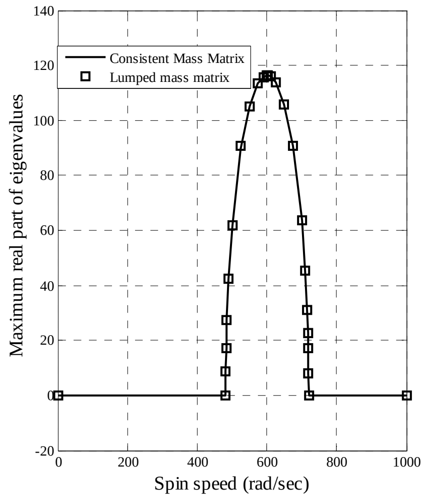

Fig. 7: Maximum real part of eigenvalues plotted against spin speed for tapered rectangular shaft with 60 mm × 40 mm cross section

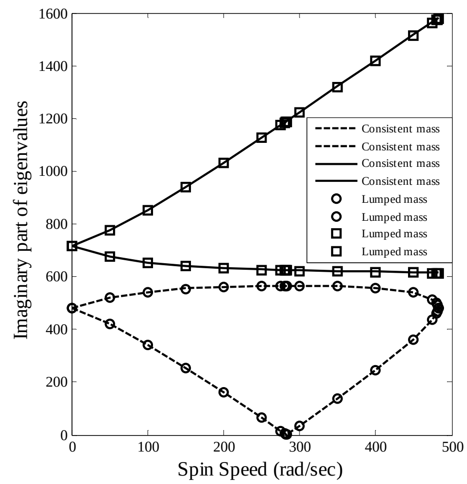

Fig. 8: Whirl speed plots vs spin speed for tapered rectangular shaft with 60 mm × 40 mm cross section

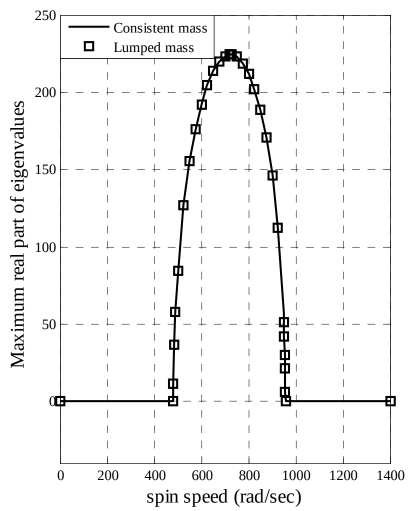

Fig. 9: Maximum real part of eigenvalues plotted against spin speed for tapered rectangular shaft with 80 mm × 40 mm cross section

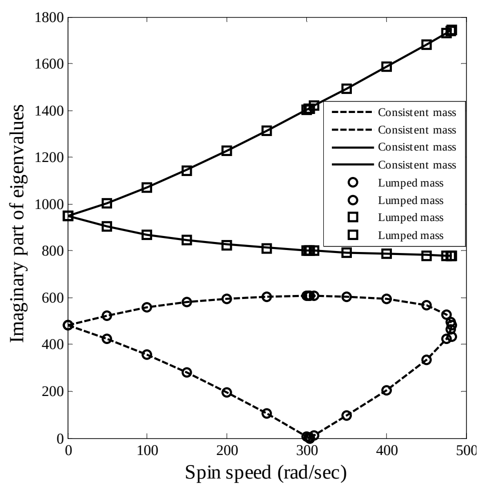

Fig. 10: Whirl speed plots vs spin speed for tapered rectangular shaft with 80 mm × 40 mm cross section

Lastly, stability analysis is performed for a cantilevered tapered asymmetrical shaft of elliptical cross section (major axis (2a): minor axis (2b) = 2:1) (Fig. 11). The length of the shaft is same as that considered in the previous cases. The cross-section tapers from a dimension a = 40 mm and b = 20 mm at the left to one with half the dimensions at the right. The smaller end is fixed. The eigenvalues are plotted in Figure 12 & Figure 13. Plots of the data from the two formulations show close proximity.

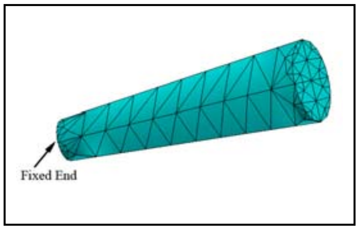

Fig. 11: Mesh idealization for tapered elliptical shaft

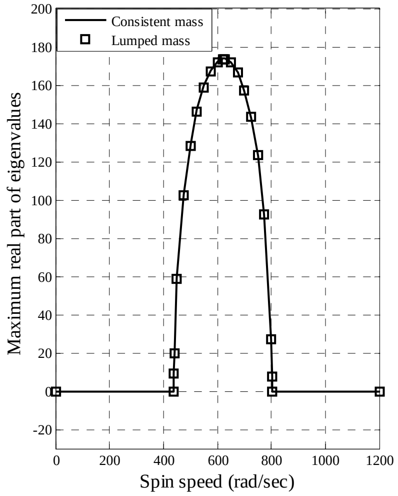

Fig. 12: Maximum real part of eigenvalues plotted against spin speed for tapered elliptical shaft

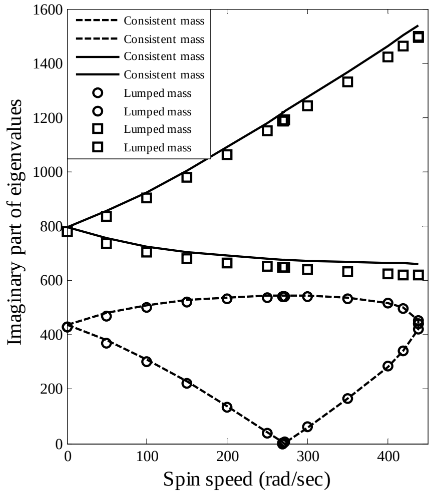

Fig. 13: Whirl speed vs spin speed plots for tapered elliptical shaft

4 Conclusion

The present work examines the performance of the well-known HRZ lumping scheme in eigenvalue analysis of rotors. This method reduces the computational effort to a large extent and found to be specially promising for shafts with unequal bending stiffness in two perpendicular planes. However, results for rotors only on rigid bearings are presented in this work. In order to have a conclusive idea about the performance of the proposed scheme, extensive numerical tests are being attempted on rotors with other types of bearings.

References

[1] H.D.Nelson, J. M. McVaugh, “The dynamics of rotor-bearing systems using finite elements”, ASME J. Eng. Ind. 98 (2) (1976) 593-600

[2] G. Genta, “Whirling of unsymmetrical rotors: a finite element approach based on complex co-ordinates”, J Sound Vib.124 (1) (1988) 27-53

[3] G. Genta, *Vibration of Structures and Machines*, Springer, New York, 1998

[4] Nandi, “On computation of response of a rotor in the deformed configuration using three-dimensional solid finite elements”, Communications in Numerical Methods in Engineering, Vol. 19, No. 3, (2003)

[5] A. Nandi, and S. Neogy, “Modelling of rotors using three-dimensional solid finite elements”, Journal of Strain Analysis for Engineering Design, Vol. 36, No. 4, (2001)

[6] E. Kramer, *Dynamics of Rotors and Foundations,* Springer, Berlin, 1990

[7] R. D. Cook, D. S. Malkus, M. E. Plesha, *Concepts and Applications of Finite Element Method,* John Wiley & Sons, New York, 1989

[8] Nandi, S. Neogy, “An efficient scheme for stability analysis of finite element asymmetric rotor models in a rotating frame”, Finite Elements Anal. Des. 41 (2005) 1343-1364